<center>═══════════ SUPERCONDUCTIVITY ═══════════</center>

# General Regularities of Magnetoresistive Effects in the Polycrystalline Yttrium and Bismuth High-Temperature Superconductor Systems

## D. A. Balaev, A. A. Bykov, S. V. Semenov, S. I. Popkov, A. A. Dubrovskii, K. A. Shaikhutdinov, and M. I. Petrov

*Kirensky Institute of Physics, Siberian Branch, Russian Academy of Sciences,*
*Akademgorodok 50, Krasnoyarsk, 660036 Russia*
*e-mail: smp@iph.krasn.ru*
Received May 25, 2010; in final form, October 1, 2010

**Abstract**—The influence of thermomagnetic prehistory on the behavior of a resistive transition $R(T)$ in external magnetic fields of polycrystalline $YBa_2Cu_3O_7$ and $Bi_{1.8}Pb_{0.3}Sr_{1.9}Ca_2Cu_3O_x$ high-temperature superconductors and the $Bi_{1.8}Pb_{0.3}Sr_{1.9}Ca_2Cu_3O_x$ + Ag texture has been investigated. It has been found that, for $YBa_2Cu_3O_7$, the thermomagnetic prehistory exerts a substantial influence on the dissipation in the subsystem of grain boundaries in magnetic fields up to $\sim 10^3$ Oe, and this effect becomes insignificant in fields higher than $\sim 10^4$ Oe. This behavior has been explained by the influence of magnetic moments of high-temperature superconductor grains on the effective magnetic field in the intergranular medium. For bismuth high-temperature superconductors, no influence of thermomagnetic prehistory on the resistive transition has been observed; however, this effect manifests itself in current–voltage characteristics at high transport current densities. There is also a radical difference in the behavior of isotherms of the magnetoresistance $R(H)$ for the yttrium and bismuth systems. For $YBa_2Cu_3O_7$, there is a clear separation between the dissipation regimes in the intergranular medium and in grains, which manifests itself even at low transport current densities as a change of sign in the curvature of the dependence $R(H)$. For a texture based on the bismuth high-temperature superconductor, this feature has been observed only at high current densities (comparable to the critical current density at $H = 0$). This difference in the behavior of magnetoresistive properties of the classical high-temperature superconductor systems under investigation has been explained by relatively low irreversibility fields of the bismuth high-temperature superconductors. In these materials, simultaneous processes of dissipation can occur in an external magnetic field both in the subsystem of grain boundaries between crystallites and in the crystallites themselves.

**DOI:** 10.1134/S1063783411050052

## 1. INTRODUCTION

Magnetoresistive effects in granular high-temperature superconductors (HTSCs) are due to the processes of penetration and redistribution of a magnetic flux in two different subsystems, i.e., superconducting grains and grain boundaries (which play the role of Josephson weak links). In external magnetic fields, dissipation occurs first of all in the subsystem of grain boundaries; however, at sufficiently high temperatures, one can observe the magnetoresistive effects associated with the flux creep or flux flow processes in HTSC grains. In turn, the magnetic moments of HTSC grains affect the intergranular medium. It is this effect that determines the hysteretic behavior of the magnetoresistance of such objects. Moreover, the magnetic properties of classical HTSC systems (for example, the yttrium and bismuth systems) also differ from each other and exhibit different anisotropies of the physical properties. Such a large diversity of factors affecting the magnetoresistive effects in granular

HTSCs makes the understanding of the physical mechanisms responsible for these phenomena difficult and impedes the elucidation of general regularities in the behavior of various granular HTSC systems. That is why the investigations of magnetoresistive phenomena in granular HTSCs, which started after the discovery of high-temperature superconductivity [1–17], have so far been performed extensively [18–25].

It is known that a sharp two-step resistive transition in magnetic fields is characteristic of the yttrium [1, 6, 7, 18–20] and lanthanum [24, 26] systems. This gave grounds to interpret the "smooth" part of the dependence $R(T)$ as being responsible for dissipation in grain boundaries and to describe experimental results in terms of the classical theories of flux creep or flux flow [6, 7, 13, 19, 20, 26–28]. However, an analysis of the experimental data available in the literature on the resistive transition in external magnetic fields for bismuth-based HTSCs [4, 5, 13, 29–37] has demonstrated that, for these objects, the dissipation regimes

in grain boundaries between crystallites and in the crystallites themselves cannot be uniquely determined.

In [12], it was shown that measurements of isotherms of the magnetoresistance for an yttrium high-temperature superconductor at temperatures close to $T_C$ revealed dissipation regimes corresponding to the subsystems of grain boundaries and HTSC crystallites. As regards the bismuth HTSC system, to the best of our knowledge, there are no data available in the literature demonstrating a similar behavior.

Moreover, although the behavior of magnetization in various HTSC systems with a different thermomagnetic prehistory is well known, the authors of the above-cited works restricted their investigations of the dependences $R(T)$ in external magnetic fields to the case of cooling in zero filed. In our opinion, the investigation of the influence of thermomagnetic prehistory for various HTSC systems and explanation of the obtained results are important problems.

It has been found that, when an external magnetic field exceeding the field of penetration into HTSC grains is turned on or off, the current–voltage characteristics of the yttrium [17] and bismuth [13] systems are determined by the influence of the magnetic flux trapped in the HTSC grains. The magnetic moments of HTSC grains affects the effective magnetic field in the intergranular medium, and it is one of the main factors limiting the critical current density of ceramic HTSCs [38]. It is this effective magnetic field that determines the magnetoresistance associated with the subsystem of grain boundaries [22, 24, 39]. The magnetization reversal of HTSC grains leads to a redistribution of the magnetic flux in the grain boundaries, which is a dominant factor responsible for the hysteresis of the magnetoresistance $R(H)$ in classical HTSC systems (such as the yttrium, bismuth, and lanthanum systems) [24]. In our opinion, the approach previously developed to adequately explain the hysteretic behavior of the magnetoresistance and critical current of granular HTSCs [22] will make it possible using available data on magnetization to explain the influence of thermomagnetic prehistory on the dependences $R(T)$ of these objects.
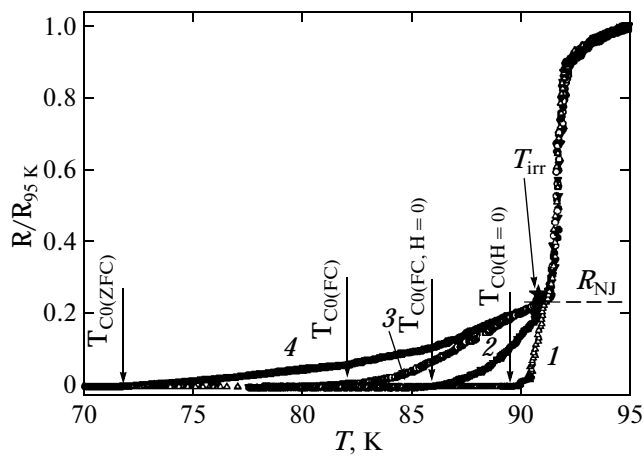
The purpose of this work was to determine the general regularities in the influence of thermomagnetic prehistory on the magnetoresistive effect and, in these measurements, to reveal the manifestation of dissipation regimes in the subsystems of grain boundaries and crystallites for classical HTSC systems (such as the yttrium and bismuth systems). The objects of our investigation were granular $YBa_2Cu_3O_7$ and $Bi_{1.8}Pb_{0.3}Sr_{1.9}Ca_2Cu_3O_x$ in the form of a texture and a polycrystal. The results were interpreted using the data obtained from magnetic measurements for the same samples.

## 2. SAMPLES AND EXPERIMENTAL TECHNIQUE

Polycrystalline high-temperature superconductors studied in this work were prepared by the solid-phase synthesis. We investigated three different series of $YBa_2Cu_3O_7$ (YBCO) samples, which differed by the time of final annealing. The absence of foreign phases in the samples was controlled using X-ray diffraction analysis. All samples had characteristics typical of the yttrium high-temperature superconductor system. In our investigations, these samples were labeled YBCO no. 1, YBCO no. 2, and YBCO no. 3. The electrical resistivity in the normal state $\rho$ (100 K), the critical current density $j_C$ (77.4 K), and the transition temperature $T_C$, which was determined from magnetic measurements and the onset of the abrupt decrease in electrical resistivity, for these samples were respectively as follows: $\approx 1.5$ mΩ cm, 80 A/cm$^2$, and 92.0 K (YBCO no. 1); $\approx 2.0$ mΩ cm, 50 A/cm$^2$, and 93.0 K (YBCO no. 2); and $\approx 1.0$ mΩ cm, 120 A/cm$^2$, and 93.0 K (YBCO no. 3). The effects engaged our attention in this work are characteristic of all the studied samples YBCO (nos. 1−3).

The technique used for preparation of the bismuth textured high-temperature superconductor with silver additions was described in [40]. The degree of texture, which was determined by the Lotgering method from X-ray diffraction data, was equal to $0.98 \pm 0.01$ [40]. The investigation of the microstructure demonstrated that the high-temperature superconductor crystallites (Bi-2223) in the form of plates with typical sizes of ~20−30 μm and a thickness of ~1 μm are ordered; the crystallographic **a**−**b** planes lie in the plate plane and the **c** axis is perpendicular to the plate plane. The measurements were performed on a sample of the composition 70 vol % $Bi_{1.8}Pb_{0.3}Sr_{1.9}Ca_2Cu_3O_x$ + 30 vol % Ag (in what follows, it will be referred to as Bi-text). For this sample, the critical current density $j_C$ (77.4 K) was equal to $\approx 220$ A/cm$^2$ and the electrical resistivity $\rho$(120 K) was $\approx 0.5$ mΩ cm. A polycrystalline sample of the composition $Bi_{1.8}Pb_{0.3}Sr_{1.9}Ca_2Cu_3O_x$ (in what follows, it will be referred to as Bi-poly) was synthesized using a procedure similar to that described in [41]. For the Bi-poly sample, the critical current density $j_C$(77.4 K) was equal to $\approx 80$ A/cm$^2$ and the electrical resistivity $\rho$(120 K) was $\approx 0.5$ mΩ cm. According to the X-ray diffraction data, the fraction of the 2221 phase for the samples Bi-text and Bi-poly was less than 5%, and the transition temperature $T_C$ determined from the magnetic measurements was 109 K.

The transport properties, current–voltage characteristics, magnetoresistance $R(H) = U(H)/I$ (where $U$ is the voltage drop and $I$ is the transport current), and dependences $R(T)$ in magnetic fields were investigated using the standard four-point probe technique. The samples were cut in the form of a parallelepiped with typical cross-sectional dimensions ~1 × 1 mm and a

**Fig. 1.** Temperature dependences $R(T)$ measured for sample YBCO no. 1 in (*I*) zero external field and (*2–4*) field $H = 150$ Oe with different thermomagnetic prehistories (*2*) FC ($H = 0$), (*3*) FC, and (*4*) ZFC. Shown are the temperatures at which "$R = 0$" ($\leq 10^{-6}$ $\Omega$ cm) for the regimes used in this work, the value of $R_{NJ}$ corresponding to the resistance of grain boundaries, and the position of the temperature $T_{irr}$ (asterisk) obtained from the data of magnetic measurements for $H = 150$ Oe (Fig. 2). The transport current is $I = 10$ mA.

length ~0.8 mm (for the Bi-text sample, the cross section was ~0.5 × 1.0 mm). The electric contacts either were pressured and gold-plated (for YBCO) or were prepared with the use of an Epo-Tek H20-E adhesive (for bismuth high-temperature superconductors). In measurements of the current–voltage characteristics and magnetoresistance $R(H)$ at $T = 77.4$ K (for the samples Bi-text and Bi-poly), the sample was placed in liquid nitrogen. This made it possible to specify the stable current up to 1 A in measurements of the magnetoresistance $R(H)$; no effects of heating the current contacts were observed. The critical current density $j_C$ was determined according to the criterion $U = 1$ μV/cm from the initial portion of the current–voltage characteristics.

The magnetic field was applied perpendicular to the direction of the transport current **j**. For the Bi-text sample, the external magnetic field was applied both parallel and perpendicular to the crystallographic **c** axis of the high-temperature superconductor crystallites. In both cases, the transport current was applied along the **a**–**b** planes of the Bi-2223 crystallites so that **j** ⊥ **H**.

The dependences $R(T)$ of the samples were measured in three different regimes of thermomagnetic prehistory: (1) zero field cooled (ZFC) measurements, establishment of a required external magnetic field, and measurements under the conditions providing heating of the sample; (2) field cooled (FC) measurements and measurements under the conditions providing heating of the sample; and (3) cooling of the sample in the magnetic field to a required tempera-

ture, decrease of the magnetic field to $H = 0$ (FC, $H = 0$), and measurements under the conditions providing heating of the sample. The current–voltage characteristics were measured only in the ZFC and FC regimes. No special measures on screening from the Earth's magnetic field were taken.

The experiments were performed on a transport properties measurement system operating at the Kirensky Institute of Physics of the Siberian Branch of the Russian Academy of Sciences (Krasnoyarsk, Russia); in some cases, the dependences $R(T)$ were measured on a Quantum Design physical properties measurement system PPMS-6000. The magnetic measurements were performed on a vibrating-sample magnetometer [42] in the regimes ZFC, FC, and FC ($H = 0$).
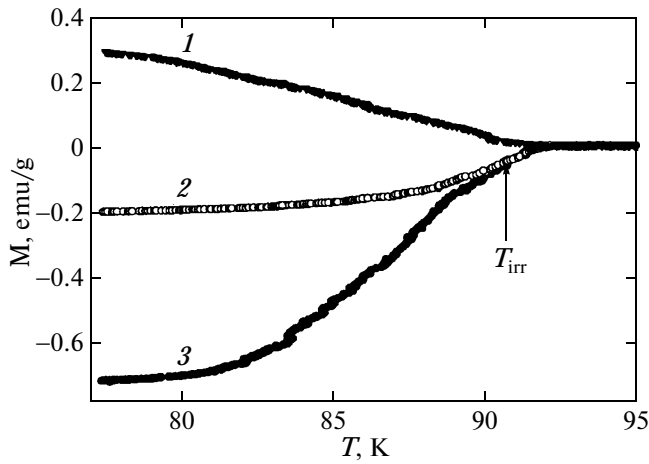
## 3. RESULTS AND DISCUSSION

### 3.1. Influence of the Thermomagnetic Prehistory of the Resistive State
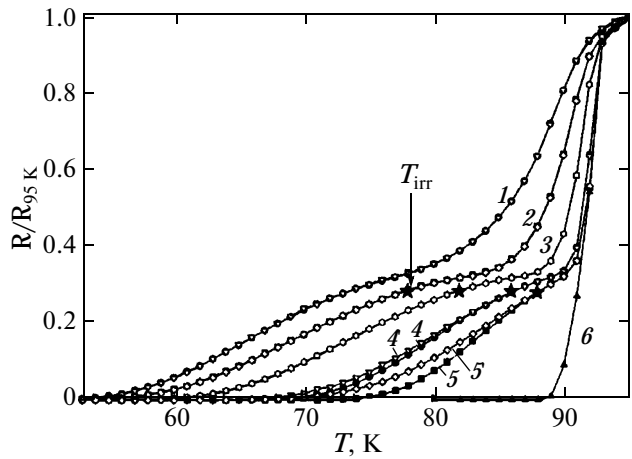
**3.1.1. Granular Y–Ba–Cu–O.** Figure 1 shows typical temperature dependences $R(T)$ measured for sample YBCO no. 1 in the external magnetic field $H = 150$ Oe with different thermomagnetic prehistories. As for the majority of weakly coupled superconductors, these dependences exhibit a two-step character, namely, an abrupt jump corresponding to the transition of superconducting grains and a smooth transition up to the temperature $T_{C0}$ (at which "$R \approx 0$" accurate to within ~$10^{-6}$ $\Omega$ cm), which is broadened in the magnetic field and determined by the Josephson junction. The quantity $R_{NJ}$ shown in Fig. 1 can be considered to be the normal resistance of the Josephson network, i.e., $R_{NJ}$, which determines the maximum magnetoresistance associated with the destruction of supercurrent carriers in grain boundaries below $T_C$ [6, 7, 27]. It can be seen from Fig. 1 that, with an increase in the temperature, the network of Josephson junctions is destroyed at a lower temperature for the ZFC case; in other words, we have $T_{C0(ZFC)} < T_{C0(FC)} < T_{C0(FC, H=0)}$ or $R_{FC(H=0)} \leq R_{FC} \leq R_{ZFC}$ (at $T = $ const).

Figure 2 shows typical temperature dependences of the magnetic moment $M(T)$ measured for sample YBCO no. 1 under the same conditions as the dependences $R(T)$ depicted in Fig. 1. These dependences are typical of high-temperature superconductors: $|M_{FC}| < |M_{ZFC}|$. The positive values of the magnetic moment $M_{FC(H=0)} > 0$ are explained by at least two factors: (1) trapping of the magnetic flux in high-temperature superconductor grains during cooling in the magnetic field and (2) processes similar to "magnetization reversal" of the type II superconductor in the absence of an applied external magnetic field [43].

The dependences $R(T)$ measured for sample YBCO no. 2 under the FC and ZFC conditions in external magnetic fields ranging from 500 Oe to
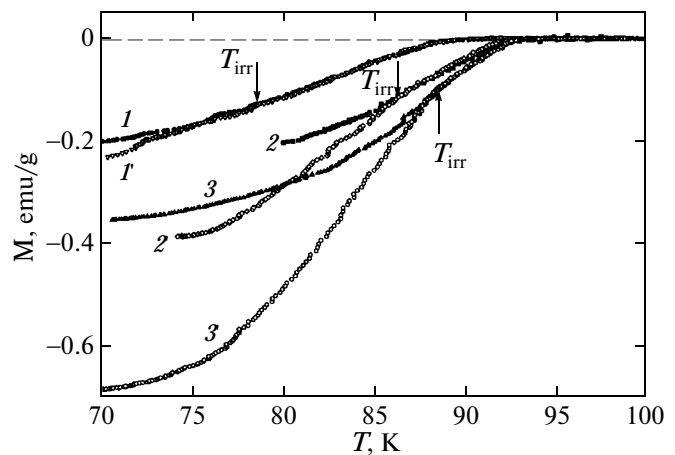
**Fig. 2.** Temperature dependences $M(T)$ measured for sample YBCO no. 1 in the external field $H = 150$ Oe with different thermomagnetic prehistories (*1*) FC ($H = 0$), (*2*) FC, and (*3*) ZFC. Shown is an example of the determination of the temperature $T_{irr}$.
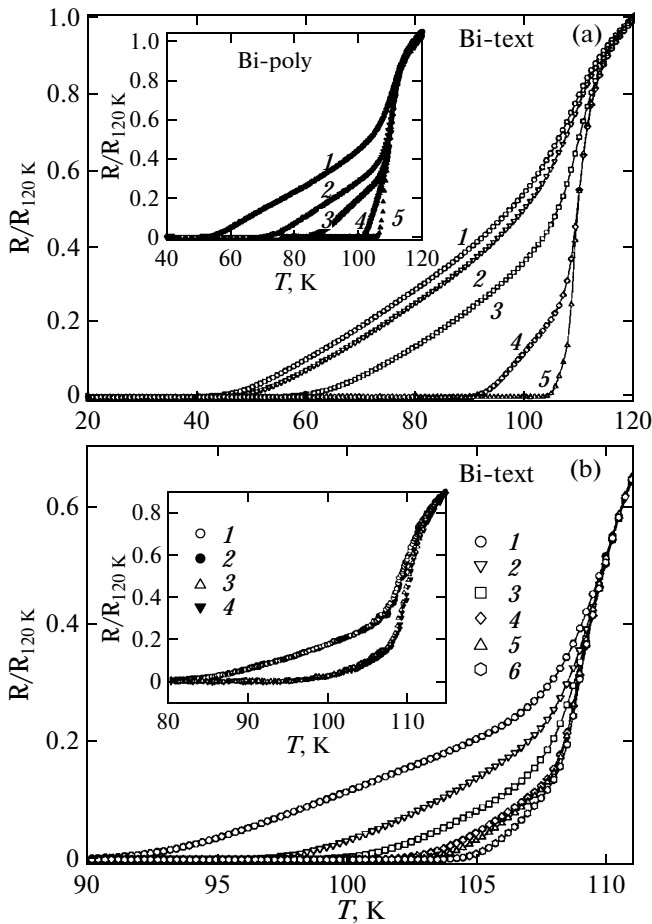


**Fig. 3.** Temperature dependences $R(T)$ measured for sample YBCO no. 2 in zero external field and different fields $H$ under the FC and ZFC conditions. $H = $ (*1*) 70, (*2*) 30, (*3*) 10, (*4*, *4'*) 2, (*5*, *5'*) 0.5, and (*6*) 0 kOe. The dependences $R(T)$ for the FC and ZFC regimes at $H \geq 10$ kOe coincide. Thermomagnetic prehistories for $H = 2.0$ and 0.5 kOe are as follows: (*4*, *5*) FC and (*4'*, *5'*) ZFC. Shown also are the positions of the temperature $T_{irr}$ (asterisks) obtained from magnetic measurements (Fig. 4) for the corresponding fields $H$. The transport current is $I = 1$ mA.

70 kOe are shown in Fig. 3. It can be seen from this figure that there are differences between the dependences $R(T)$ measured in the FC and ZFC regimes for magnetic fields $H = 500$ Oe and $H = 2$ kOe; however, in external magnetic fields of ~10 kOe and higher, the differences between the dependences $R(T)$ disappear. Figure 4 shows typical temperature dependences of the magnetization $M(T)$ measured for sample YBCO no. 2 also under the FC and ZFC conditions in magnetic fields of 500 Oe, 2 kOe, and 3 kOe. The temperature, at which the dependences $M(T)$ FC and $M(T)$ ZFC for the same value of magnetic field $H$ begin to coincide with each other, is defined as the temperature of the irreversible behavior of magnetization, i.e., $T_{irr}$, and this value of the field is referred to as the irreversibility field $H_{irr}$ at the given temperature [43]. Examples of the determination of the temperature $T_{irr}$ are shown in Figs. 2 and 4. The positions of the $T_{irr}$ points (obtained from magnetic measurements) with respect to the dependences $R(T)$ (FC and ZFC) for the corresponding values of the external magnetic field are presented in Figs. 3 and 1, respectively.

For relatively low magnetic fields of 150 and 500 Oe, the values of $T_{irr}$ are identical to temperatures above which the dependences $R(T)$ FC and $R(T)$ ZFC coincide. In the magnetic field $H = 2$ kOe, the dependences $R(T)$ FC and $R(T)$ ZFC begin to coincide well before the onset of the temperature $T_{irr}$ corresponding to the magnetic measurements. For higher magnetic fields, no influence of the thermomagnetic prehistory on the dependences $R(T)$ was revealed and the $T_{irr}$ point lies in the temperature range corresponding to dissipation at grain boundaries (the smooth "tail" of the dependences $R(T)$).

In order to explain the observed difference in the behavior of the dependences $R(T)$ measured under conditions with thermomagnetic prehistories used in this work, we invoke the model of a granular high-temperature superconductor, which was proposed for adequately describing the $R(H)$ hysteresis of these objects in our previous paper [22]. It is known that an external magnetic field of the order of a few oersteds (or lesser) already percolates into grain boundaries [8, 44]. The magnetic induction lines induced by magnetic moments of high-temperature superconductor grains



**Fig. 4.** Temperature dependences $M(T)$ measured for sample YBCO no. 2 in different external fields $H = $ (*1*, *1'*) 30, (*2*, *2'*) 2, and (*3*, *3'*) 0.5 kOe with different thermomagnetic prehistories (*1*–*3*) FC and (*1'*–*3'*) ZFC.

**Fig. 5.** Temperature dependences $R(T)$ measured for the Bi-text sample at $\mathbf{H} \parallel \mathbf{c}$ in (a) zero external field and (b) fields up to 1 kOe. $H =$ (a) (*1*) 80, (*2*) 60, (*3*) 20, (*4*) 1, and (*5*) 0 and (b) (*1*) 1.0, (*2*) 0.3, (*3*) 0.1, (*4*) 0.03, (*5*) 0.01, and (*6*) 0 kOe. The inset in panel (a) shows the dependences $R(T)$ for the Bi-poly sample at $H =$ (*1*) 60, (*2*) 10, (*3*) 2, (*4*) 0.35, and (*5*) 0 kOe. The transport current is $I = 1$ mA for all graphs, except those shown in the inset to panel (b). Within the limits of the experimental error, the data obtained for the FC and ZFC regimes coincide for all graphs shown in the figure. In the inset to panel (b), this is illustrated for the dependences $R(T)$ of the Bi-text sample at $\mathbf{H} \parallel \mathbf{c}$ in external fields $H =$ (*1*, *2*) 3 kOe and (*3*, *4*) 300 Oe with different thermomagnetic prehistories (*1*, *3*) ZFC and (*2*, *4*) FC. $I = 30$ mA.

also close up through the intergranular space. If the magnetic moment has a negative value (i.e., it is directed opposite to the external field), the direction of the magnetic induction lines from the magnetic moments of the grains in the region of grain boundaries coincides with the direction of the external magnetic field [22].[1] Therefore, the grain boundaries (or the Josephson medium) are in an effective magnetic field $B_{\text{eff}}$, which represents a superposition of the

---

[1] The schematic diagram illustrating the magnetic induction lines in the intergranular medium is presented in the corresponding figures in [22, 23].

external and induced fields. This induced field can be considered as being proportional to the magnetic moment of the sample [22–24]; hence, taking into account the sign of the quantity $M(H)$, we can write

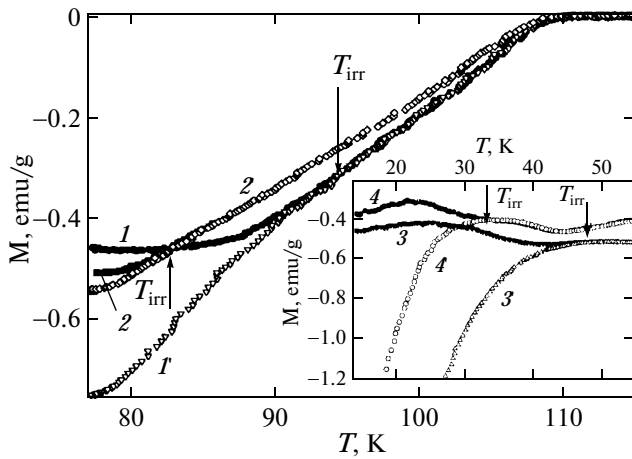$$B_{\text{eff}}(H) = H + 4\pi\alpha(H)M(H), \tag{1}$$

where $\alpha(H)$ includes the flux distribution inside the grains, their effective demagnetization factor, geometric parameters of the grains, etc.[2] We can abstract away from the processes of trapping of the magnetic flux inside the grains (process FC) or flux redistribution (process (FC, $H = 0$)) and, in the subsequent analysis, will operate with the magnetic moment of the sample (obviously, it is a superposition of magnetic moments of individual grains [46]): $|M_{\text{ZFC}}| > |M_{\text{FC}}|$ at $T < T_{\text{irr}}$; therefore, we can write $B_{\text{eff(ZFC)}} > B_{\text{eff(FC)}}$. For the FC regime ($H = 0$), we have $B_{\text{eff(FC } H = 0)} \sim M$ (in this case, the direction of the induced magnetic field is of no importance, because $H = 0$). From this consideration it follows that, at $T < T_{\text{irr}}$, $B_{\text{eff(ZFC)}} > B_{\text{eff(FC } H = 0)}$.

In the case where the dissipation occurs only in grain boundaries, the magnetoresistance is determined by the effective magnetic field $B_{\text{eff}}$, It is clear that $R \sim B_{\text{eff}}$. This consideration explains the difference in the behavior of the dependences $R(T)$ in the studied regimes (Figs. 1, 3). At $T > T_{\text{irr}}$, the dependences $R(T)$ should coincide, which is actually observed in the range of weak fields (Figs. 1, 3). In strong external magnetic fields, the induced field (the second term in expression (1)) has already not introduce a noticeable contribution to the effective field ($B_{\text{eff}} \approx H$). Therefore, in the range of fields higher than $H \sim 10$ kOe, no difference is observed in the behavior of the dependences $R(H)$ for the FC and ZFC regimes (Fig. 3). Moreover, with an increase in the temperature, the difference $|M_{\text{ZFC}} - M_{\text{FC}}|$ also decreases (Figs. 2, 4). Consequently, the values of $B_{\text{eff}}$ for the FC and ZFC regimes also become close to each other as the temperature $T_{\text{irr}}$ is approached. This manifests itself in the experimental dependences $R(T)$ at $H = 500$ Oe and $H = 2$ kOe (Fig. 3). The difference between the dependences $R(T)$ for the FC and ZFC regimes becomes indistinguishable at $T \approx 87$ and $\approx 82$ K, whereas the values of $T_{\text{irr}}$ for this sample are equal to $\approx 88$ and $\approx 86$ K, respectively.

**3.1.2. Texture and the Bi–Ca–Sr–Cu–O (2223) crystal.** A different pattern is observed for the bismuth-based texture. The temperature dependences $R(T)$ measured for the Bi-text sample in magnetic fields from 0 to 80 kOe for the field orientation $\mathbf{H} \parallel \mathbf{c}$ (where $\mathbf{c}$ is the crystallite axis) are shown in Fig. 5. As can be seen from this figure, the data on the dependences $R(T)$ obtained for the FC and ZFC regimes coincide

---

[2] The evaluation of the parameter $\alpha$ was performed in [24, 39, 45]. In this paper, we have restricted ourselves to the qualitative explanation of the behavior of the dependence $R(T)$ in different regimes.
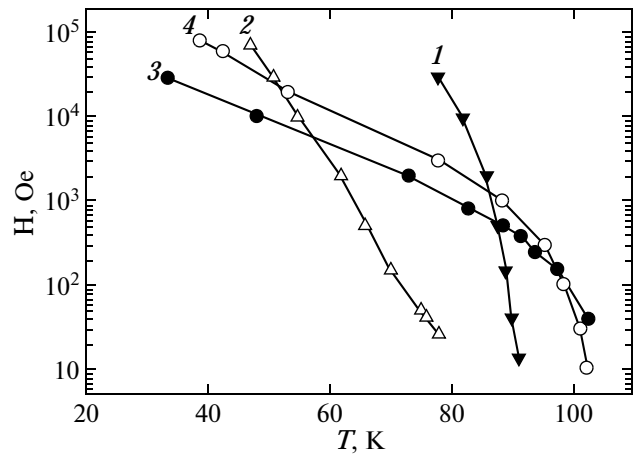
**Fig. 6.** Typical temperature dependences $M(T)$ measured for the Bi-text sample at $\mathbf{H} \parallel \mathbf{c}$ in external fields $H = (1, 1')$ 240 and $(2, 2')$ 700 Oe with different thermomagnetic prehistories $(1, 2)$ FC and $(1', 2')$ ZFC. The inset shows fragments of the dependences $M(T)$ in external fields $H = (3, 3')$ 10 and $(4, 4')$ 30 kOe with thermomagnetic prehistories $(3, 4)$ FC and $(3', 4')$ ZFC.
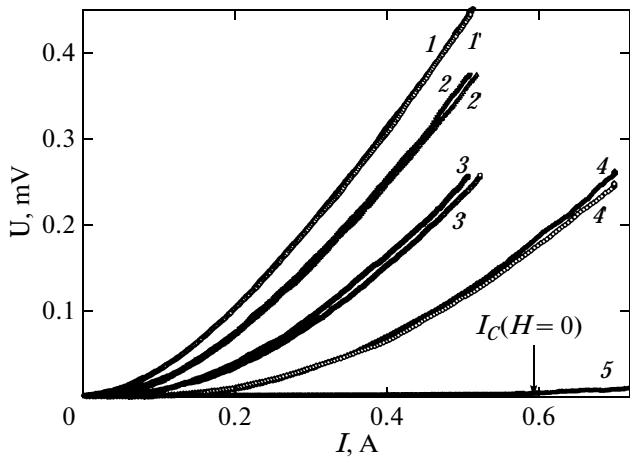
**Fig. 7.** Behavior of $(1, 3)$ the irreversibility line $H_{irr}(T)$ (field $H$ for which the temperature $T_{irr}$ was determined (see Figs. 4, 6)) and $(2, 4)$ the dependences $T_{C0(ZFC)}(H)$ under the ZFC conditions (an example of the determination is shown in Fig. 1) in the $H-T$ coordinates: $(1, 2)$ sample YBCO no. 2 and $(3, 4)$ sample Bi-text at $\mathbf{H} \parallel \mathbf{c}$.

both in the range of high magnetic fields and in magnetic fields below 1 kOe. It is worth noting that this coincidence is observed both for the transport current $I = 1$ mA and for higher values of $I$ (this is clearly illustrated in the inset to Fig. 5b for fields $H = 300$ Oe and 3 kOe at $I = 30$ mA). A similar behavior (when there is no difference in the behavior of the dependences $R(T)$ for the FC and ZFC regimes) is also observed for the Bi-poly sample (see the dependences $R(T)$ shown in the inset to Fig. 5a).

This behavior can be understood by considering the behavior of the irreversibility line $H_{irr}(T)$ and the temperature $T_{C0}$ (which was introduced above; see Fig. 1) in the $H-T$ coordinates. Typical temperature dependences $M(T)$ measured for the Bi-text sample in the FC and ZFC regimes for the field orientation $\mathbf{H} \parallel \mathbf{c}$ and examples of the determination of the temperature $T_{irr}$ for different values of $H$ are presented in Fig. 6.

Figure 7 shows the dependences $H_{irr}(T)$ plotted in the $\log H-T$ coordinates (where $H_{irr}$ is the external magnetic field for which the temperature $T_{irr}$ was determined (see Figs. 2, 4, 6)) and the dependences $T_{C0(ZFC)}(H)$ for the samples Bi-text (orientation $\mathbf{H} \parallel \mathbf{c}$, Fig. 5 for the current $I = 1$ mA) and YBCO no. 2 (for the data presented in Fig. 3). As can be seen from Fig. 7, there is a radical difference in the behavior of the dependences $H_{irr}(T)$ for the bismuth and yttrium high-temperature superconductors, which is typical of the studied systems [47, 48]. Noteworthy also are the relative positions of the irreversibility lines $H_{irr}(T)$ and the dependences $T_{C0(ZFC)}(H)$. For the YBCO sample, the dependence $T_{C0(ZFC)}(H)$ plotted in the $H-T$ coordinates always lies below the irreversibility line $H_{irr}(T)$: $T_{C0(ZFC)} < T_{irr}$ at $H = $ const. A different behavior is

observed for the Bi-text sample. Almost over the entire temperature region (except for the narrow range above $\approx 100$ K), the values of $T_{C0}$ are higher than those of $T_{irr}$ for a given field $H$. According to our data, this behavior is characteristic of the field orientation $\mathbf{H} \parallel \mathbf{a}-\mathbf{b}$.

For the yttrium system, there is a rather wide temperature range between $T_{C0}$ and $T_{irr}$ at $H = $ const. It is in this range that the effects of the influence of the thermomagnetic prehistory (FC and ZFC) on the dependence $R(T)$ are observed in the experiment. It should be noted that this range corresponds to the part of the dependence $R(T)$ responsible for the dissipation in the subsystem of grain boundaries (Figs. 1, 3). For the bismuth system, the temperature dependences $M(T)$ in the FC and ZFC regimes begin to coincide at a temperature below $T_{C0}$ (which corresponds to the onset of the dissipation). Although the dependences $R(T)$ for the bismuth systems in external magnetic fields have been investigated in many works (see, for example, [4, 5, 29−37]), this fact has not been noted previously. We can conclude that, for the bismuth system in external magnetic fields at relatively low current densities (which have been usually used in measurements of the dependences $R(T)$), both the weak links at grain boundaries and the high-temperature superconductor crystallites themselves simultaneously transform into the resistive state.

However, the effects of thermomagnetic prehistory in transport current measurements can also be observed when the subsystem of weak links in an external magnetic field lower than the irreversibility field $H_{irr}$ is purposefully transformed by the transport current into the resistive state. In other words, for this purpose, it is necessary to perform measurements of
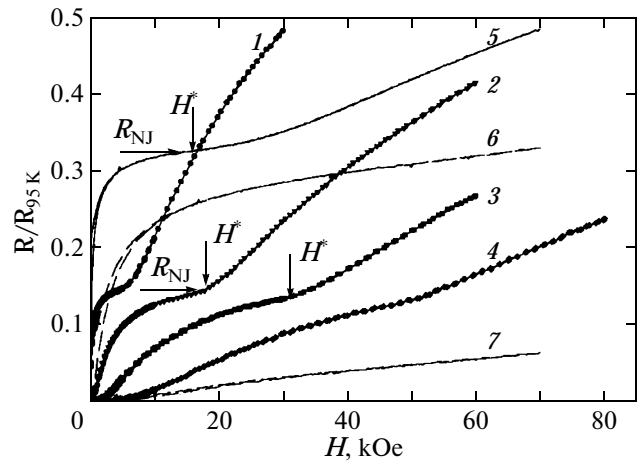
**Fig. 8.** Current–voltage characteristics measured for the Bi-text sample in different external fields (**H** ∥ **c**) at $T = 77.4$ K with different thermomagnetic prehistories (*1–4*) FC, (*1'–4'*) ZFC, and (*5*) without an applied field. $H = ($*1*, *1'*$)$ 700, ($2$, $2'$) 375, ($3$, $3'$) 240, and ($4$, $4'$) 40 Oe. Shown is the current $I_C$ $(H = 0)$.



**Fig. 9.** Field dependences $R(H)$ measured for samples (*1–4*) YBCO no. 3 and (*5–7*) YBCO no. 2 at different temperatures $T = ($*1*$)$ 90, ($2$) 87.5, ($3$, $5$) 85.0, ($4$) 82.5, ($6$) 77.4, and ($6$) 60 K. The measurement current is $I = 1$ mA. Shown are the values of $R_{NJ}$ and the points $H^*$ at which the curvature of the dependences $R(H)$ changes sign. The data on the dependences $R(H)$ are normalized to the resistance of the sample at $T = 95$ K.
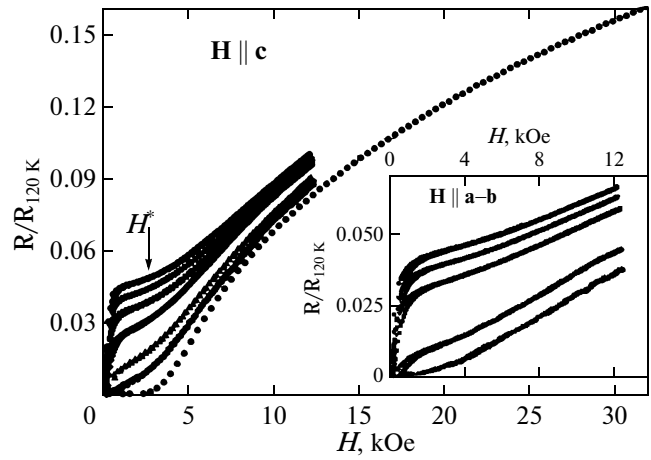
the current–voltage characteristics in the FC and ZFC regimes. Figure 8 shows the current–voltage characteristics measured for the Bi-text sample in different external fields (orientation **H** ∥ **c**) at $T = 77.4$ K in the FC and ZFC regimes. The values of $H$ and the orientation of **H** and **c** for the data presented in Fig. 8 are identical to those used for the magnetic measurements illustrated in Fig. 6. It can be seen that the magnetoresistance measured in the ZFC regime is higher than that obtained in the FC regime, as is observed in the case with the YBCO sample. In the field $H = 700$ Oe, this effect becomes almost imperceptible, because the difference $|M_{ZFC} - M_{FC}|$ at $T = 77.4$ K decreases (Fig. 6) and its influence on the effective magnetic field in the intergranular medium, which is determined by expression (1), becomes insignificant. For the Bi-poly sample, we obtained similar results.

### 3.2. Contribution to Magnetoresistance from Grain Boundaries and Crystals. Difference in the Behavior of the Yttrium and Bismuth Systems

For the YBCO sample, the contribution from the subsystem of grain boundaries is clearly seen in the dependences $R(T)$: it is a smooth part of the dependence $R(T)$ in weak fields (Fig. 1). The value of $R$ at the inflection point of the curve $R(T)$ in strong fields (Fig. 3) corresponds to the resistance of the Josephson network in the "normal" state, i.e., $R_{NJ}$. The two-step transition to the superconducting state, which is observed in measurements of the dependences $R(T)$ in external magnetic fields, also manifests itself in the isotherms $R(H)$. Figure 9 shows the field dependences $R(H)$ measured for samples YBCO no. 2 and YBCO no. 3 at different temperatures. When the tempera-

tures are significantly different from $T_C$, the dissipation occurs only in grain boundaries and the dependences $R(H)$ demonstrate a tendency toward saturation (see the data presented in Fig. 9 for sample YBCO no. 2 at temperatures $T = 60.0$ and 77.4 K). With an increase in the temperature, the dependences $R(H)$ begin to exhibit a specific feature, i.e., an inflection point at $H = H^*$. In this case, the dependences $R(H)$ to the left of the point $H^*$ are determined by the dissipation in grain boundaries, whereas to the right of this point, they are most likely determined by the dissipation in high-temperature superconductor grains. This can be seen from the data obtained for samples YBCO no. 2 ($T = 85$ K) and YBCO no. 3 (Fig. 9). A change of the sign in the curvature of the dependences $R(H)$ corresponds to a crossover from the regime of dissipation in grain boundaries to the regime of dissipation in grains. The resistance $R_{NJ}$, i.e., the value of $R$ at the inflection point, is the "maximum" magnetoresistance of the subsystem of weak links. This can be judged from a comparison of the dependences $R(T)$ (Fig. 3) and $R(H)$ (Fig. 9a) measured for sample YBCO no. 2.[3] It should be noted that the data presented in Figs. 1, 3, and 9 (for YBCO) were obtained at relatively low transport current densities ($j = 0.1–1.0$ A/cm², $I = 1–10$ mA), which are considerably less than the value of $j_C$ (77.4 K, $H = 0$). At higher transport current densities, the aforementioned features in the dependences $R(T)$ and $R(H)$ are more pronounced.

---

[3] The dependences $R(H)$ in the vicinity of the temperature $T_C$ (which have a similar inflection point) were investigated earlier in detail only for the $Y_{1-x}Pr_xBa_2Cu_3O_7$ ($x = 0.35$) system [12].

Thus, for the yttrium system in external magnetic fields, there is a clear boundary between the dissipation processes: first, weak links at grain boundaries completely transform into the resistive state; and, then, with increasing magnetic field, the dissipation occurs in crystallites.

The dependences $R(H)$[4] measured for the Bi-text sample at $T = 77.4$ K, the field orientation $\mathbf{H} \parallel \mathbf{c}$, and different values of the transport current are shown in Fig. 10. The range of variations in the transport current includes values lower than the critical current in the absence of an external magnetic field ($I_c(77.4$ K$) \approx 600$ mA) and values higher than the critical current. For a low measurement current $I = 1$ mA, the dependence $R(H)$ is a conventional $S$-shaped curve, which is characteristic of type II superconductors. The measurements performed using the Bi-text sample ($\mathbf{H} \parallel \mathbf{c}$) with a low transport current $I = 1$ mA at other temperatures (up to $T_C$) also did not reveal remarkable features. The "two-phase" property of the system, which manifests itself in a tendency toward saturation and, then, with an increase in the external magnetic field, toward a change of the sign in the curvature of the dependence $R(H)$, is observed only at a transport current $I \geq 200$ mA. At $I = 0.8-1.0$ A, the dependences $R(H)$ for the Bi-text sample are actually similar to the dependences $R(H)$ for the yttrium system. A change of the sign in the curvature of the curves $R(H)$ takes place at $H^* \sim 2$ kOe ($\mathbf{H} \parallel \mathbf{c}$); incidentally, this value of $H^*$ is close to the value of $H_{\mathrm{irr}}$ at $T = 77$ K (Fig. 7). For the field orientation $\mathbf{H} \parallel \mathbf{a}-\mathbf{b}$, the dependences $R(H)$ also demonstrate the aforementioned features (see the inset to Fig. 10), and the change of the sign in the curvature of the curves $R(H)$ takes place at $H^* \sim 4$ kOe. An increase in $R(H)$ in fields above 4 kOe occurs more slowly than in the case of $\mathbf{H} \parallel \mathbf{c}$. Such anisotropy of the magnetoresistive properties is inherent in the textures based on the bismuth high-temperature superconductor and was discussed earlier in [29, 49, 50].

To the best of our knowledge, up to now, there have been no experimental data available in the literature, according to which the dependences $R(H)$ for bismuth high-temperature superconductors (textures or polycrystals; see, for example, [4, 5, 29, 31, 32, 50]) demonstrate such remarkable features. These features have been observed under the conditions where the transport current is comparable to $I_C(H = 0)$ at a given temperature. For relatively low transport currents (1–100 mA for the data presented in Fig. 10), the dissipation in the range of weak fields, as in the case of granular YBCO, arises from the decay of carriers upon tunneling through grain boundaries. However, in the field $H^*$, at which the magnetoresistance appears in Bi-



**Fig. 10.** Field dependences $R(H)$ measured for the Bi-text sample at $T = 77.4$ K, $\mathbf{H} \parallel \mathbf{c}$, and different values of the measurement current $I = 1000, 800, 600, 400, 200, 100,$ and 1 mA (from top to bottom). Shown is the field $H^*$ at which the curvature of the dependences $R(H)$ changes sign at high currents $I$. The inset presents the dependences $R(H)$ for the Bi-text sample at $T = 77.4$ K, $\mathbf{H} \parallel \mathbf{a}-\mathbf{b}$, and different measurement currents $I = 1000, 800, 600, 200,$ and 100 mA (from top to bottom). The data on the dependences $R(H)$ are normalized to the resistance of the sample at $T = 120$ K.

2223 crystallites, the magnetoresistance of the subsystem of grain boundaries is still far short of saturation. For $H > H^*$, the dissipation processes occur both in crystallites and in grain boundaries. Consequently, a sharp increase in the magnetoresistance at $H \sim H^*$ is not observed. A relatively high transport current transforms the subsystem of grain boundaries into the resistive state at a lower value of the external magnetic field (or at $H = 0$ when $I > I_C(H = 0)$). Hence, the dependence $R(H)$ exhibits a tendency toward saturation only at sufficiently high transport currents $I$. In this case, the appearance of dissipation in crystallites at $H \sim H^*$ is well pronounced in the dependence $R(H)$. For the yttrium system, this behavior manifests itself at sufficiently low transport currents (Fig. 9).

The observed difference in the magnetoresistive properties of these classical high-temperature superconductors can be interpreted as follows. For YBCO, the Josephson coupling energy, which characterizes the subsystem of grain boundaries, is considerably less than the corresponding characteristic of the YBCO grains; in other words, we have $J_{\mathrm{CJ}} \ll J_{\mathrm{CG}}$ (the subscripts J and G corresponds to the Josephson medium and grains, respectively). The same is also true for the Bi-2223 system; however, the strong condition $J_{\mathrm{CJ}} \ll J_{\mathrm{CG}}$ is not satisfied in external magnetic fields. This is explained by the difference in the behavior of the irreversibility lines for YBCO and Bi-2223 (Fig. 7). Despite the lower value of $T_C$, the fields $H_{\mathrm{irr}}$ for the yttrium system are one order of magnitude higher than those for Bi-2223 with the field orientation $\mathbf{H} \parallel \mathbf{c}$

---

[4] In the range of fields below $H^*$, at which the curvature of the dependence $R(H)$ changes sign, the magnetoresistance exhibits a hysteresis (it is clearly seen in Figs. 9 and 10). The factors responsible for this hysteresis were thoroughly discussed in [22–24].

already at a temperature of ~80 K. This behavior of the irreversibility line is known and was discussed in [49]. It is these relatively low values of the irreversibility field for the Bi-2223 system that are responsible for the observed difference in the behavior of the magnetoresistive properties of Bi-2223 and YBCO. In external magnetic fields of the order of $H_{irr}$, the dissipation processes can occur both in the subsystem of grain boundaries and in the Bi-2223 crystallites.

The above property of the Bi-2223 system also manifests itself in the fact that, in external magnetic fields, there is a difference between the shapes of the dependences $R(T)$ of this system and the YBCO system. For YBCO, we can clearly separate the contribution from the grain boundaries and their resistance in the normal state, i.e., $R_{NJ}$ (Fig. 3). For the B-text sample, it is impossible to reveal a portion of the dependence $R(T)$ that corresponds to the contribution from a particular subsystem (Fig. 5). Incidentally, this is true for both the high-field range 20−80 kOe (Fig. 5a) and the field range $H \leq 1$ kOe (Fig. 5b). The value of $R$, at which after the sharp drop of the resistance there appears a smooth part of the dependence $R(T)$, increases with an increase in the external magnetic field. This behavior is characteristic of not only the textured high-temperature superconductor but also polycrystalline high-temperature superconductors based on bismuth [30−37] (see also the inset to Fig. 5a).

Another factor that affects the appearance of specific features in the dependences $R(H)$, which correspond to the onset of dissipation in Bi-2223 crystallites, is the anisotropy of the crystallites themselves. For the field orientation $\mathbf{H} \parallel \mathbf{a}-\mathbf{b}$, the change of sign in the curvature of the dependence $R(H)$ is less pronounced (see the inset to Fig. 10); furthermore, the value of $H^*$ is higher than that for the field orientation $\mathbf{H} \parallel \mathbf{c}$. For a chaotic orientation of crystallites in the bismuth high-temperature superconductor polycrystal, it should be expected that this feature will be at least diffuse. Our measurements have demonstrated that, for the aforementioned polycrystal, this feature is not observed in the dependences $R(H)$. The dependences $R(H)$ for this polycrystal are ascending curves similar to the dependences $R(H)$ for sample YBCO no. 2 at temperatures $T = 77.4$ and $60.0$ K in Fig. 10. The used values of the transport current (50−400 mA) were both lower and higher than the critical current of this sample in the absence of an external magnetic field ($I_C(77.4 \text{ K}) \approx 270$ mA, $j_C(77.4 \text{ K}) \approx 80$ A/cm$^2$), which is comparable to relative values of the transport current in measurements of the dependences $R(H)$ for the Bi-text sample (Fig. 10). Moreover, we investigated the dependences $R(H)$ at $T = 77.4$ K for the $Bi_{1.8}Pb_{0.3}Sr_{1.9}Ca_2Cu_3O_x$ sample with a low density (the sample preparation and the microstructure are described in [34]), in which plate-like Bi-2223 crystallites are also chaotically oriented. Up to the values of the transport current, which are one order of magnitude higher than the critical current at $H = 0$, no features are observed in the dependences $R(H)$. Therefore, we can assume that, for polycrystalline Bi-2223, the absence of a characteristic point corresponding to the change of sign in the curvature of the curves $R(H)$ is associated with the influence of anisotropy of the crystallites.

## 4. CONCLUSIONS

The yttrium-based granular high-temperature superconductors and bismuth-based textures investigated in this work exhibit an identical behavior in the influence of thermomagnetic prehistory on the resistive state. The obtained results have been explained in the framework of the previously developed model of a granular high-temperature superconductor [22]. In this model, we have considered the influence of the magnetic moments of high-temperature superconductor grains on the effective magnetic field in the intergranular medium. The effects associated with the influence of thermomagnetic prehistory on the magnetoresistive properties are determined by different contributions from the magnetic moments of superconducting grains to this effective field, and the influence of thermomagnetic prehistory itself is more significant in the range of weak fields.

This has introduced serious corrections to the interpretation of the previously obtained results for granular high-temperature superconductors. In a number of works [4−7, 14], the processing of experimental temperature dependences of the resistive transition in the framework of the models developed for weakly coupled superconductors made it possible to obtain the field dependence of the pinning potential in a Josephson medium, which has been discussed in terms of theoretical concepts. Even in the case of cooling in zero field, the external magnetic field does not correspond to the effective field $B_{eff}$ defined by expression (1). Only for external magnetic fields of the order of $10^4$ Oe did we obtain $B_{eff} \approx H$. Therefore, the field dependence of the pinning potential in the Josephson medium of a granular high-temperature superconductor in the range of weak fields should be interpreted taking into account the correction of the effective magnetic field.

The revealed difference in the influence of thermomagnetic prehistory on the behavior of the resistive transition for the yttrium and bismuth systems has been explained by lower values of the irreversibility fields of the bismuth high-temperature superconductors. This is also responsible for the specific features observed in the isotherms of the magnetoresistance of the textured bismuth-based high-temperature superconductor samples. In particular, the dependences $R(H)$ obtained for granular YBCO samples clearly exhibit regimes of dissipation both in grain boundaries

(the range of weak fields) and in high-temperature superconductor crystallites (the range of intermediate or strong fields depending on whether the temperature is farther from or closer to $T_C$), whereas this behavior for the Bi-2223 textures is observed only at a transport current density $j$ of the order of $j_C$ ($H = 0$). In view of the relatively low irreversibility fields of the bismuth high-temperature superconductors, the processes of dissipation at low current densities in external magnetic fields $H \geq H_{irr}$ occur simultaneously in the subsystem of grain boundaries and in the Bi-2223 crystallites themselves. This is a fundamental difference between the ratios of the intergrain and intragrain critical current densities in external magnetic fields for the classical high-temperature superconductor systems under investigation. Moreover, for the bismuth polycrystal, characteristic features of the dependences $R(H)$ (such as the change of sign in the curvature of the dependence upon crossover from the regime of dissipation in grain boundaries to the regime of dissipation in crystallites) have not been observed even in the measurements performed at transport current densities of the order of $j_C$ ($H = 0$). This is associated with the influence of anisotropy of the magnetoresistive properties of the Bi-2223 crystallites.

Classical high-temperature superconductor systems, such as the Bi-2223, thallium-based ($Tl_2Ba_2Ca_2Cu_3O_y$ (Tl-2223)), and mercury-based ($Hg_2Ba_2Ca_2Cu_3O_8$ (Hg-2223)) systems, possess a stronger anisotropy of the critical parameters as compared to the YBCO and lanthanum-based (($La,Sr)_2CuO_4$ (LSCO)) systems. It is also known that the pinning and its related irreversibility fields of the aforementioned classes of high-temperature superconductors are maximum for the YBCO and LSCO systems [48]. The behavior of the dependences $R(T)$ in external magnetic fields for polycrystalline high-temperature superconductors Tl-2223 and Hg-2223, which is known from the literature [51, 52], is similar to that observed for the bismuth high-temperature superconductor. Therefore, it should be expected that the effects of thermomagnetic prehistory (FC, ZFC) also will not affect the dependences $R(T)$ for these strongly anisotropic high-temperature superconductor systems and that the isotherms of the magnetoresistance $R(H)$ can clearly exhibit regimes of dissipation in grain boundaries and in crystallites only for textured objects. On the other hand, the polycrystalline LSCO samples demonstrate a sharp two-step resistive transition in a magnetic field [24, 26]. Therefore, for this system, we can expect that the influence of the FC and ZFC regimes on the resistive transition, as well as the character of the dependences $R(H)$, will be similar to that observed for granular YBCO samples.

## REFERENCES

1. M. A. Dubson, S. T. Herbert, J. J. Calabrese, D. C. Harris, B. R. Patton, and J. C. Garland, Phys. Rev. Lett. **60** (11), 1061 (1988).

2. V. L. Kozhevnikov, K. R. Krylov, A. I. Ponomarev, M. V. Sadovskii, I. M. Tsidil'kovskii, and S. M. Cheshnitskii, Fiz. Met. Metalloved **64** (1), 184 (1987).

3. Y. J. Quian, Z. M. Tang, K. Y. Chen, B. Zhou, J. W. Qui, B. C. Miao, and Y. M. Cai, Phys. Rev. B: Condens. Matter **39** (7), 4701 (1989).

4. A. C. Wright, K. Zhang, and A. Erbil, Phys. Rev. B: Condens. Matter **44** (2), 863 (1991).

5. A. C. Wright, T. K. Xia, and A. Erbil, Phys. Rev. B: Condens. Matter **45** (2), 5607 (1992).

6. C. Gaffney, H. Petersen, and R. Bednar, Phys. Rev. B: Condens. Matter **48** (5), 3388 (1993).

7. H. S. Gamchi, G. J. Russel, and K. N. R. Taylor, Phys. Rev. B: Condens. Matter **50** (17), 12950 (1994).

8. D. N. Kuz'michev, Pis'ma Zh. Eksp. Teor. Fiz. **74** (5), 291 (2001) [JETP Lett. **74** (5), 262 (2001)].

9. I. Felner, E. Galstyan, B. Lorenz, D. Cao, Y. S. Wang, Y. Y. Xue, and C. W. Chu, Phys. Rev. B: Condens. Matter **67**, 134506 (2003).

10. D. Daghero, P. Mazzetti, A. Stepanesku, P. Tura, and A. Masoero, Phys. Rev. B: Condens. Matter **66**, 184514 (2002).

11. P. Muné, F. C. Fonseca, R. Muccillo, and R. F. Jardim, Physica C (Amsterdam) **390** (4), 363 (2003).

12. C. A. M. dos Santos, M. S. da Luz, B. Ferriera, and A. J. S. Machado, Physica C (Amsterdam) **391** (4), 345 (2003).

13. E. Govea-Alcaide, R. F. Jardim, and P. Muné, Physica C (Amsterdam) **423** (3–4), 152 (2005).

14. M. R. Mohammadizadeh and M. Akhavan, Supercond. Sci. Technol. **16**, 538 (2003).

15. A. A. Sukhanov and V. I. Omelchenko, Fiz. Nizk. Temp. (Kharkov) **29** (4), 396 (2003) [Low Temp. Phys. **29** (4), 297 (2003)].

16. A. A. Sukhanov and V. I. Omelchenko, Fiz. Nizk. Temp. (Kharkov) **30** (6), 604 (2004) [Low Temp. Phys. **30** (6), 452 (2004)].

17. V. V. Derevyanko, T. V. Sukhareva, and V. A. Finkel', Fiz. Tverd. Tela (St. Petersburg) **48** (8), 1374 (2006) [Phys. Solid State **48** (8), 1455 (2006)].

18. C. A. M. dos Santos, C. J. V. Oliveira, M. S. da Luz, A. D. Bortolozo, M. J. R. Jardim, and A. J. S. Machado, Phys. Rev. B: Condens. Matter **74**, 184526 (2006).

19. G. L. Bhalla and Pratima, Supercond. Sci. Technol. **20**, 1120 (2007).

20. A. Gupta, A. J. Deshpande, V. P. S. Awana, S. Balamurugan, K. N. Sood, R. Kishore, H. Kishan, E. Takayama-Muromachi, and A. V. Narlikar, Supercond. Sci. Technol. **20**, 1084 (2007).

21. T. V. Sukhareva and V. A. Finkel', Fiz. Tverd. Tela (St. Petersburg) **50** (6), 961 (2008) [Phys. Solid State **50** (6), 1001 (2008)].

22. D. A. Balaev, D. M. Gokhfeld, A. A. Dubrovskii, S. I. Popkov, K. A. Shaikhutdinov, and M. I. Petrov, Zh. Eksp. Teor. Fiz. **132** (6) 1340 (2007) [JETP **105** (6), 1174 (2007)].

23. D. A. Balaev, A. A. Dubrovskii, S. I. Popkov, K. A. Shaikhutdinov, and M. I. Petrov, Fiz. Tverd. Tela (St. Petersburg) **50** (6), 972 (2008) [Phys. Solid State **50** (6), 1014 (2008)].

24. D. A. Balaev, A. A. Dubrovskii, K. A. Shaikhutdinov, S. I. Popkov, D. M. Gokhfeld, Yu. S. Gokhfeld, and M. I. Petrov, Zh. Eksp. Teor. Fiz. **135** (2), 271 (2009) [JETP **108** (2), 241 (2009)].

25. T. V. Sukhareva and V. A. Finkel, Zh. Eksp. Teor. Fiz. **134** (5), 922 (2008) [JETP **107** (5), 787 (2008)].

26. L. Urba, C. Acha, and V. Bekeris, Physica C (Amsterdam) **279**, 92 (1997).

27. D. A. Balaev, S. I. Popkov, K. A. Shaikhutdinov, and M. I. Petrov, Fiz. Tverd. Tela (St. Petersburg) **48** (5), 780 (2006) [Phys. Solid State **48** (5), 826 (2006)].

28. D. K. Mani, M. Zouaoui, M. Annabi, F. B. Azzouz, and M. B. Salem, J. Phys.: Conf. Ser. **97**, 012182 (2008).

29. G. C. Han and C. K. Ong, Phys. Rev. B: Condens. Matter **56** (17), 11299 (1997).

30. D. G. Marinaro, J. Horvat, S. X. Dou, I. Kusecic, E. Babic, R. Weinstein, and A. Gandini, Supercond. Sci. Technol. **15**, 1596 (2002).

31. M. Ionescu, B. Winton, T. Silver, S. X. Dou, and R. Ramer, J. Phys. D: Appl. Phys. **37**, 1727 (2004).

32. B. Winton, M. Ionescu, T. Silver, and S. X. Dou, J. Phys. D: Appl. Phys. **38**, 2327 (2005).

33. M. Pekala, H. Bougrine, T. Lada, A. Morawski, and M. Ausloos, Supercond. Sci. Technol. **8**, 726 (1995).

34. K. A. Shaikhutdinov, D. A. Balaev, S. I. Popkov, and M. I. Petrov, Supercond. Sci. Technol. **20** (6), 491 (2007).

35. M. H. Pu, Z. S. Cao, Q. Y. Wang, and Y. Zhao, Supercond. Sci. Technol. **19**, 462 (2006).

36. A. V. Pop, R. Deltour, A. H. Harabor, D. Ciurchea, Gh. Ilonca, V. Pop, and M. Todica, Supercond. Sci. Technol. **10**, 843 (1997).

37. R. K. Nkum and W. R. Datars, Supercond. Sci. Technol. **8**, 822 (1995).

38. Kh. R. Rostami, Zh. Eksp. Teor. Fiz. **134** (4), 716 (2008) [JETP **107** (4), 612 (2008)].

39. K. A. Shaikhutdinov, D. A. Balaev, S. I. Popkov, and M. I. Petrov, Fiz. Tverd. Tela (St. Petersburg) **51** (6), 1046 (2009) [Phys. Solid State **51** (6), 1105 (2009)].

40. M. I. Petrov, I. L. Belozerova, K. A. Shaikhutdinov, D. A. Balaev, A. A. Dubrovskii, S. I. Popkov, A. D. Vasil'ev, and O. N. Mart'yanov, Supercond. Sci. Technol. **21**, 105 019 (2008).

41. V. S. Kravchenko, M. A. Zhuravleva, E. M. Uskov, P. P. Bezverkhnii, N. A. Bogolyubov, O. G. Potapova, and L. L. Makarshin, Neorg. Mater. **34** (10), 1274 (1998) [Inorg. Mater. **34** (10), 1074 (1998)].

42. A. D. Balaev, Yu. V. Boyarshinov, M. M. Karpenko, and B. P. Khrustalev, Prib. Tekh. Eksp., No. 3, 167 (1985).

43. D. M. Ginsberg, in *Physical Properties of High Temperature Superconductors I*, Ed. by D. M. Ginsberg (World Scientific, Singapore, 1989; Mir, Moscow, 1990), p. 69.

44. E. B. Sonin, Pis'ma Zh. Eksp. Teor. Fiz. **47** (8), 415 (1988) [JETP Lett. **47** (8), 496 (1988)].

45. M. N. Kunchur and T. R. Askew, J. Appl. Phys. **84** (12), 6763 (1998).

46. V. V. Val'kov and B. P. Khrustalev, Zh. Eksp. Teor. Fiz. **107** (4), 121 (1995) [JETP **80** (4), 680 (1995)].

47. Y. Xu and M. Suenaga, Phys. Rev. B: Condens. Matter **43** (7), 5516 (1991).

48. L. F. Cohen and H. J. Jensen, Rep. Prog. Phys. **60**, 1581 (1997).

49. B. Lehndorff, M. Hortig, and H. Piel, Supercond. Sci. Technol. **11**, 1261 (1998).

50. G. C. Han, H. M. Han, Z. H. Wang, X. N. Liu, W. F. Yuan, and F. T. Wang, Phys. Rev. B: Condens. Matter **51** (18), 12754 (1995).

51. J. D. Hettinger, A. D. Swanson, J. C. Brooks, J. Z. Huang, L. Q. Chen, and Zh. Zhao, Supercond. Sci. Technol. **1**, 349 (1989).

52. J. Roa-Rojas, P. Pureur, L. Mendocca-Ferreira, M. T. D. Orlando, and E. Baggio-Saitovitch, Supercond. Sci. Technol. **14**, 898 (2001).

*Translated by O. Borovik-Romanova*